

**The impact of patch forwarding on the prevalence of computer virus  
A theoretical assessment approach**

Yang, Lu Xing; Yang, Xiaofan; Wu, Yingbo

**DOI**

[10.1016/j.apm.2016.10.028](https://doi.org/10.1016/j.apm.2016.10.028)

**Publication date**

2017

**Document Version**

Final published version

**Published in**

Applied Mathematical Modelling

**Citation (APA)**

Yang, L. X., Yang, X., & Wu, Y. (2017). The impact of patch forwarding on the prevalence of computer virus: A theoretical assessment approach. *Applied Mathematical Modelling*, 43, 110-125.  
<https://doi.org/10.1016/j.apm.2016.10.028>

**Important note**

To cite this publication, please use the final published version (if applicable).  
Please check the document version above.

**Copyright**

Other than for strictly personal use, it is not permitted to download, forward or distribute the text or part of it, without the consent of the author(s) and/or copyright holder(s), unless the work is under an open content license such as Creative Commons.

**Takedown policy**

Please contact us and provide details if you believe this document breaches copyrights.  
We will remove access to the work immediately and investigate your claim.



# The impact of patch forwarding on the prevalence of computer virus: A theoretical assessment approach



Lu-Xing Yang<sup>a,b,\*</sup>, Xiaofan Yang<sup>a</sup>, Yingbo Wu<sup>a</sup>

<sup>a</sup>School of Software Engineering, Chongqing University, Chongqing 400044, China

<sup>b</sup>Faculty of Electrical Engineering, Mathematics and Computer Science, Delft University of Technology, GA, Delft 2600, The Netherlands

## ARTICLE INFO

### Article history:

Received 14 January 2016

Revised 31 August 2016

Accepted 11 October 2016

Available online 2 November 2016

### Keywords:

Computer virus

Virus patch

Node-level epidemic model

Equilibrium

Global stability

Spectral radius

## ABSTRACT

Virus patches can be disseminated rapidly through computer networks and take effect as soon as they have been installed, which significantly enhances their virus-containing capability. This paper aims to theoretically assess the impact of patch forwarding on the prevalence of computer virus. For that purpose, a new malware epidemic model, which takes into full account the influence of patch forwarding, is proposed. The dynamics of the model is revealed. Specifically, besides the permanent susceptible equilibrium, this model may admit an infected or a patched or a mixed equilibrium. Criteria for the global stability of the four equilibria are given, respectively, accompanied with numerical examples. The obtained results show that the spectral radii of the patch-forwarding network and the virus-spreading network both have a marked impact on the prevalence of computer virus. The influence of some key factors on the prevalence of virus is also revealed. Based on these findings, some strategies of containing electronic virus are recommended.

© 2016 Elsevier Inc. All rights reserved.

## 1. Introduction

The malware epidemic dynamics has been recognized as an effective approach to the assessment of prevalence of computer virus [1]. Since Kephart and White's seminal work [2], a multitude of malware epidemic models, ranging from simple models [3–10] to advanced models such as delayed models [11,12], impulsive models [13–15] and stochastic models [16,17], have been proposed.

Patches targeting malware can be disseminated through technological networks (such as the Internet, the world-wide web, and online social networks) to a large fraction of network nodes at an extremely high velocity. Moreover, the patch dissemination can be carried out in a distributed way (every node that was newly patched tries to forward the patches to all of its neighbors), so as to reduce the overhead of network resources. For the purpose of theoretically assessing the effectiveness of the patch forwarding strategy, Yang and Yang [18,19] suggested two malware epidemic models taking into account the influence of patch forwarding. As the models assume that every node is either susceptible or infected or patched, they are referred to as the Susceptible-Infected-Patched models, abbreviated as the SIPS models. The distinction between the two models lies in that the first model ignores the influence of infected removable storage media, whereas the second model considers that influence. The two SIPS models are both compartmental, that is, all nodes are grouped into three compartments according to their current states, and the major concern is the change in the fraction of each

\* Corresponding author at: School of Software Engineering, Chongqing University, Chongqing 400044, China.

E-mail addresses: [ylx910920@gmail.com](mailto:ylx910920@gmail.com) (L.-X. Yang), [xfyang1964@gmail.com](mailto:xfyang1964@gmail.com) (X. Yang), [wyb@cqu.edu.cn](mailto:wyb@cqu.edu.cn) (Y. Wu).

compartment. As these SIPS models cannot accommodate the complete information concerning the network structures, in most situations the effectiveness of the patch-forwarding strategy cannot be accurately assessed by studying them. For related work on this topic, see Refs. [20–24].

What node-level epidemic models mean are epidemic models that accommodate the probability of every node being in a state. As node-level epidemic models can accommodate the full knowledge concerning the network topology, the impact of the network topology on the prevalence of virus can be revealed by studying such models. In 2009, Mieghem et al. [25] introduced the first node-level epidemic model by remoulding a traditional SIS model. Later, Xu et al. [26] proposed a node-level SIR model capturing the dynamics of multivirus. By introducing the added alert state, Sahneh and Scoglio [27] established a node-level SAIS model. It was found under these epidemic models that the spectral radius of the virus-spreading network plays a key role in determining the virus prevalence [25–27]. For more information on this topic, see Refs. [28–32]. In the context of patch forwarding, viruses propagate through the virus-spreading network, whereas patches are disseminated through the patch-forwarding network, and the two networks may be different. Consequently, it is of practical importance to study the combined impact of the patch-forwarding network and the virus-spreading network on the viral prevalence. To our knowledge, however, there is yet no report in literature on this topic.

This paper addresses the theoretical assessment of the patch forwarding strategy. For that purpose, a node-level SIPS model, which takes into full account the influence of the patch forwarding, is proposed. The dynamics of the model is revealed. Specifically, besides the permanent susceptible equilibrium, this model may admit an infected or a patched or a mixed equilibrium. Criteria for the global stability of the four equilibria are given, respectively, accompanied with numerical examples. The obtained results show that the spectral radii of the patch-forwarding network and the virus-spreading network both have a marked impact on the prevalence of computer virus. The influence of some key factors on the prevalence of virus is also revealed. Based on these findings, some virus-containing policies are recommended.

The remaining materials of this paper are organized in this pattern: Section 2 formulates the new malware epidemic model. Section 3 theoretically analyzes the proposed model, and Section 4 illustrates the obtained results. Section 5 examines the impact of some factors on the virus prevalence and thereby draws some new insights on containing virus spreading. Finally, Section 6 summarizes this work and points out some directions of research.

## 2. Formation of a node-level SIPS model

Consider a networked system of  $N$  nodes labeled  $1, 2, \dots, N$ . Let  $V = \{1, 2, \dots, N\}$ . Let  $G_v = (V, E_v)$  denote the virus-propagating network, where two nodes are adjacent if and only if computer viruses can propagate directly from one of them to the other. Let  $\mathbf{A} = [a_{ij}]_{N \times N}$  denote the adjacency matrix of  $G_v$ , and let  $\rho(\mathbf{A})$  denote the spectral radius of  $\mathbf{A}$ , which equals its maximum eigenvalue. Let  $G_p = (V, E_p)$  denote the patch-forwarding network, where two nodes are adjacent if and only if patches can be forwarded directly from one of them to the other. Let  $\mathbf{B} = [b_{ij}]_{N \times N}$  denote the adjacency matrix of  $G_p$ , and let  $\rho(\mathbf{B})$  denote the spectral radius of  $\mathbf{B}$ , which equals its maximum eigenvalue. In what follows, it is always assumed that the virus-spreading network and the patch-forwarding network are both connected.

As with the compartmental SIPS models [18,19], it is assumed in the new model that at any time, each and every node in the system is in one of three states: *susceptible*, *infected*, and *patched*. A node is susceptible if it is uninfected and with no newest patches. Hence, a susceptible node can be infected by an infected  $G_v$ -neighbor or patched by a patched  $G_p$ -neighbor. In contrast, a node is patched if it is not only uninfected but with newest patches. As a result, a patched node cannot be infected by an infected  $G_v$ -neighbor. Finally, an infected node is with no newest patches and hence can be patched by a patched  $G_p$ -neighbor.

Let  $S_i(t)$ ,  $I_i(t)$ , and  $P_i(t)$  denote the probability that at time  $t$ , node  $i$  is susceptible, infected, and patched, respectively. Clearly, the vector

$$\tilde{\mathbf{x}}(t) = (S_1(t), \dots, S_N(t), I_1(t), \dots, I_N(t), P_1(t), \dots, P_N(t))^T,$$

probabilistically captures the  $t$ -time state of the system. Let

$$\tilde{\Omega} = \{(S_1, \dots, S_N, I_1, \dots, I_N, P_1, \dots, P_N)^T \in \mathbb{R}_+^{3N} \mid S_i + I_i + P_i = 1, i = 1, 2, \dots, N\}.$$

Then  $\tilde{\mathbf{x}}(t) \in \tilde{\Omega}$  for all  $t \geq 0$ .

As  $S_i(t) + I_i(t) + P_i(t) \equiv 1, 1 \leq i \leq N$ , the vector

$$\mathbf{x}(t) = (I_1(t), \dots, I_N(t), P_1(t), \dots, P_N(t))^T,$$

also probabilistically captures the  $t$ -time state of the system. Let

$$\Omega = \{(I_1, \dots, I_N, P_1, \dots, P_N)^T \in \mathbb{R}_+^{2N} \mid I_i + P_i \leq 1, i = 1, 2, \dots, N\}.$$

Then  $\mathbf{x}(t) \in \Omega$  for all  $t \geq 0$ . In what follows, let  $\overset{\circ}{\Omega}$  and  $\partial\Omega$  denote the interior and boundary of  $\Omega$ , respectively.

Now, let us impose a set of statistical assumptions on the state transition of a node as follows.

- (H1) Due to the propagation of viruses, a susceptible node is infected by an infected  $G_v$ -neighbor at a constant rate  $\beta > 0$ . At the early stage of invasion of viruses, a susceptible node  $i$  gets infected at time  $t$  approximately at rate  $\beta \sum_j a_{ij} I_j(t)$ .

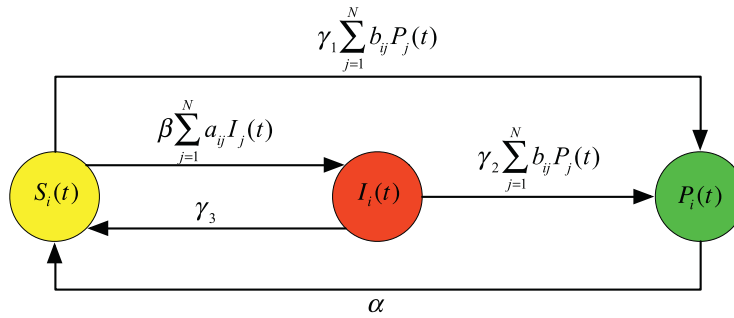


Fig. 1. Diagram of assumptions (H1)–(H4).

- (H2) Due to the dissemination of newest patches, a susceptible (respectively, infected) node is patched by a patched \$G\_p\$-neighbor at a constant rate \$\gamma\_1 > 0\$ (respectively, \$\gamma\_2 > 0\$). At the early stage of release of new patches, a susceptible (respectively, infected) node \$i\$ gets patched at time \$t\$ approximately at rate \$\gamma\_1 \sum\_j b\_{ij} P\_j(t)\$ (respectively, \$\gamma\_2 \sum\_j b\_{ij} P\_j(t)\$).
- (H3) Due to the reinstallation of the operating system, a infected node becomes susceptible at a constant rate \$\gamma\_3 > 0\$.
- (H4) Due to the loss of efficacy of old patches, a patched node becomes susceptible at a constant rate \$\alpha > 0\$.

Fig. 1 shows these assumptions schematically.

Let \$\Delta t\$ be a very small time interval. Assumptions (H1)–(H4) imply that the probabilities of state transition of node \$i\$ satisfy the following relations.

$$\Pr(i \text{ is infected at time } t + \Delta t \mid i \text{ is susceptible at time } t) = \beta \Delta t \sum_j a_{ij} I_j(t) + o(\Delta t),$$

$$\Pr(i \text{ is patched at time } t + \Delta t \mid i \text{ is susceptible at time } t) = \gamma_1 \Delta t \sum_j b_{ij} P_j(t) + o(\Delta t),$$

$$\Pr(i \text{ is susceptible at time } t + \Delta t \mid i \text{ is infected at time } t) = \gamma_3 \Delta t + o(\Delta t),$$

$$\Pr(i \text{ is patched at time } t + \Delta t \mid i \text{ is infected at time } t) = \gamma_2 \Delta t \sum_j b_{ij} P_j(t) + o(\Delta t),$$

$$\Pr(i \text{ is susceptible at time } t + \Delta t \mid i \text{ is patched at time } t) = \alpha \Delta t + o(\Delta t).$$

Invoking the total probability formula and letting \$\Delta t \to 0\$, we get a dynamical model as follows.

$$\begin{cases} \frac{dS_i(t)}{dt} = \alpha P_i(t) + \gamma_3 I_i(t) - \beta S_i(t) \sum_j a_{ij} I_j(t) - \gamma_1 S_i(t) \sum_j b_{ij} P_j(t), & i = 1, 2, \dots, N, \\ \frac{dI_i(t)}{dt} = -\gamma_3 I_i(t) + \beta S_i(t) \sum_j a_{ij} I_j(t) - \gamma_2 I_i(t) \sum_j b_{ij} P_j(t), & i = 1, 2, \dots, N, \\ \frac{dP_i(t)}{dt} = -\alpha P_i(t) + \gamma_1 S_i(t) \sum_j b_{ij} P_j(t) + \gamma_2 I_i(t) \sum_j b_{ij} P_j(t), & i = 1, 2, \dots, N, \end{cases} \quad (1)$$

with \$\tilde{\mathbf{x}}(0) \in \tilde{\Omega}\$.

As \$S\_i(t) + I\_i(t) + P\_i(t) \equiv 1, 1 \le i \le N\$, model (1) is equivalent to the following reduced dynamical model.

$$\begin{cases} \frac{dI_i(t)}{dt} = -\gamma_3 I_i(t) + \beta(1 - I_i(t) - P_i(t)) \sum_j a_{ij} I_j(t) - \gamma_2 I_i(t) \sum_j b_{ij} P_j(t), & i = 1, 2, \dots, N, \\ \frac{dP_i(t)}{dt} = -\alpha P_i(t) + \gamma_1(1 - I_i(t) - P_i(t)) \sum_j b_{ij} P_j(t) + \gamma_2 I_i(t) \sum_j b_{ij} P_j(t), & i = 1, 2, \dots, N, \end{cases} \quad (2)$$

with \$\mathbf{x}(0) \in \Omega\$. This model can be rewritten in matrix notation as

$$\frac{d\mathbf{x}(t)}{dt} = \mathbf{F}(\mathbf{x}(t)), \quad \mathbf{x}(0) \in \Omega. \quad (3)$$

The above three models are equivalent. In what follows, we shall refer to model (2) as the *node-level SIPS model*. This model has the following basic property.

**Lemma 1.** \$\Omega\$ is positively invariant for model (2). That is, \$\mathbf{x}(0) \in \Omega\$ implies \$\mathbf{x}(t) \in \Omega\$ for all \$t > 0\$.

**Proof.** \$\partial\Omega\$ consists of the following \$3N\$ hyperplanes:

$$H_i = \{(I_1, \dots, I_N, P_1, \dots, P_N)^T \in \Omega \mid I_i = 0\}, \quad 1 \le i \le N,$$

$$H_{N+i} = \{(I_1, \dots, I_N, P_1, \dots, P_N)^T \in \Omega \mid P_i = 0\}, \quad 1 \le i \le N,$$

$$H_{2N+i} = \{(I_1, \dots, I_N, P_1, \dots, P_N)^T \in \Omega \mid I_i + P_i = 1\}, \quad 1 \le i \le N.$$

For  $1 \leq i \leq N$ ,  $H_i$ ,  $H_{N+i}$ , and  $H_{2N+i}$  have

$$\mathbf{n}_i = (0, \dots, 0, \underbrace{-1}_i, 0, \dots, 0)^T,$$

$$\mathbf{n}_{N+i} = (0, \dots, 0, \underbrace{-1}_{N+i}, 0, \dots, 0)^T,$$

and

$$\mathbf{n}_{2N+i} = (0, \dots, 0, \underbrace{1}_i, 0, \dots, 0, \underbrace{1}_{N+i}, 0, \dots, 0)^T,$$

as their respective outer normal vectors. Let  $\hat{\mathbf{x}} = (\hat{I}_1, \dots, \hat{I}_N, \hat{P}_1, \dots, \hat{P}_N)^T$  be a smooth point of  $\partial\Omega$ . We distinguish among three possibilities.

Case 1: Some  $\hat{I}_i = 0$ . Then,  $\langle \mathbf{F}(\hat{\mathbf{x}}), \mathbf{n}_i \rangle = -\beta(1 - \hat{P}_i) \sum_j a_{ij} \hat{I}_j \leq 0$ .

Case 2: Some  $\hat{P}_i = 0$ . Then,  $\langle \mathbf{F}(\hat{\mathbf{x}}), \mathbf{n}_{N+i} \rangle = -\gamma_1(1 - \hat{I}_i) \sum_j b_{ij} \hat{P}_j - \gamma_2 \hat{I}_i \sum_j b_{ij} \hat{P}_j \leq 0$ .

Case 3: Some  $\hat{I}_i + \hat{P}_i = 1$ . Then,  $\langle \mathbf{F}(\hat{\mathbf{x}}), \mathbf{n}_{2N+i} \rangle = -\gamma_3 \hat{I}_i - \alpha \hat{P}_i < 0$ .

Combining the above discussions, we get that  $\mathbf{F}(\hat{\mathbf{x}})$  is pointing to  $\Omega$ . The claim follows from Ref. [33]. □

### 3. Analysis of the node-level SIPS model

This section aims to understand the dynamics of model (2) proposed in the previous section.

#### 3.1. Equilibria

The first step to study the dynamics of model (2) is to examine its equilibria. For that purpose, let us introduce the following definition.

**Definition 1.** Let  $\mathbf{E} = (I_1, \dots, I_N, P_1, \dots, P_N)^T$  be an equilibrium of model (2).

- (a)  $\mathbf{E}$  is *susceptible* if  $I_1 = \dots = I_N = P_1 = \dots = P_N = 0$ .
- (b)  $\mathbf{E}$  is *infected* if some  $I_i > 0$  and  $P_1 = \dots = P_N = 0$ .
- (c)  $\mathbf{E}$  is *patched* if some  $P_i > 0$  and  $I_1 = \dots = I_N = 0$ .
- (d)  $\mathbf{E}$  is *mixed* if some  $I_i > 0$  and some  $P_j > 0$ .

Obviously, model (2) always admits a unique susceptible equilibrium  $\mathbf{E}_s = (0, \dots, 0, 0, \dots, 0)^T$ . The following theorem gives criteria for the existence of the other three kinds of equilibria of model (2), respectively.

**Theorem 1.** Consider model (2). The following claims hold.

- (a) If  $\rho(\mathbf{A}) > \frac{\gamma_3}{\beta}$ , then there is a unique infected equilibrium, denoted  $\mathbf{E}_i = (I_1^*, \dots, I_N^*, 0, \dots, 0)^T$ . Moreover,  $0 < I_i^* < 1$ ,  $1 \leq i \leq N$ .
- (b) If  $\rho(\mathbf{B}) > \frac{\alpha}{\gamma_1}$ , then there is a unique patched equilibrium, denoted  $\mathbf{E}_p = (0, \dots, 0, P_1^*, \dots, P_N^*)^T$ . Moreover,  $0 < P_i^* < 1$ ,  $1 \leq i \leq N$ .
- (c) Suppose  $\gamma_1 = \gamma_2$ . If  $\rho(\mathbf{B}) > \frac{\alpha}{\gamma_1}$  and  $\rho(\mathbf{A}) > \max_i \left\{ \frac{\alpha P_i^* + \gamma_3(1 - P_i^*)}{\beta(1 - P_i^*)^2} \right\}$ , then there is a unique mixed equilibrium, denoted  $\mathbf{E}_m = (I_1^{**}, \dots, I_N^{**}, P_1^{**}, \dots, P_N^{**})^T$ . Moreover,  $P_i^{**} = P_i^*$ ,  $0 < I_i^{**} < 1 - P_i^*$ ,  $1 \leq i \leq N$ .

**Proof.** (a) Suppose model (2) admits an infected equilibrium  $\mathbf{E} = (I_1, \dots, I_N, 0, \dots, 0)^T$ . We show that  $0 < I_i < 1$ ,  $1 \leq i \leq N$ . It follows from model (2) that

$$I_i = \frac{\beta \sum_j a_{ij} I_j}{\gamma_3 + \beta \sum_j a_{ij} I_j} < 1, \quad 1 \leq i \leq N.$$

On the contrary, suppose that some  $I_k = 0$ . It follows from model (2) that  $\sum_j a_{kj} I_j = 0$ . As  $G_V$  is connected, we get that some  $a_{kl} = 1$ , implying that  $I_l = 0$ . Repeating this argument, we finally get that  $I_i = 0$ ,  $1 \leq i \leq N$ , contradicting the assumption that  $\mathbf{E}$  is an infected equilibrium. Hence,  $I_i > 0$ ,  $1 \leq i \leq N$ .

Define a continuous mapping as follows.

$$\mathbf{H} = (h_1, \dots, h_N) : (0, \infty)^N \rightarrow (0, 1)^N,$$

$$h_i(\mathbf{x}) = \frac{\beta \sum_j a_{ij} x_j}{\gamma_3 + \beta \sum_j a_{ij} x_j}, \quad \mathbf{x} = (x_1, \dots, x_N)^T \in (0, \infty)^N, \quad 1 \leq i \leq N.$$

It suffices to show that  $\mathbf{H}$  admits a unique fixed point. To this end, we first prove the following claim.

**Claim 1.**  $\mathbf{H}$  is monotonic.

**Proof of Claim 1.** Let  $\mathbf{x}, \mathbf{y} \in (0, \infty)^N$ ,  $\mathbf{x} \leq \mathbf{y}$  (i.e.,  $x_i \leq y_i$ ,  $1 \leq i \leq N$ ). Then,

$$h_i(\mathbf{x}) = \frac{\beta \sum_j a_{ij} x_j}{\gamma_3 + \beta \sum_j a_{ij} x_j} \leq \frac{\beta \sum_j a_{ij} y_j}{\gamma_3 + \beta \sum_j a_{ij} y_j} = h_i(\mathbf{y}), \quad 1 \leq i \leq N,$$

which implies  $\mathbf{H}(\mathbf{x}) \leq \mathbf{H}(\mathbf{y})$ . Claim 1 is proved. □

It is well known that the connectedness of  $G_V$  implies the irreducibility of  $\mathbf{A}$ . According to the Perron–Frobenius Theorem [34],  $\rho(\mathbf{A}) > 0$  is a simple eigenvalue of  $\mathbf{A}$ , and  $\rho(\mathbf{A})$  has a positive eigenvector  $\mathbf{v} = (v_1, \dots, v_N)^T$ . Let

$$\varepsilon_1 = \left[ 1 - \frac{\gamma_3}{\rho(\mathbf{A})} \right] \cdot \frac{1}{\max_i \{v_i\}}, \quad \varepsilon_2 = \left[ 1 - \frac{\gamma_3}{\rho(\mathbf{A})} \right] \cdot \frac{1}{\min_i \{v_i\}}.$$

Then,  $0 < \varepsilon_1 \leq \varepsilon_2$ . Thus,

$$h_i(\varepsilon_1 \mathbf{v}) = \frac{\beta \varepsilon_1 \sum_j a_{ij} v_j}{\gamma_3 + \beta \varepsilon_1 \sum_j a_{ij} v_j} = \frac{\beta \varepsilon_1 v_i \rho(\mathbf{A})}{\gamma_3 + \beta \varepsilon_1 v_i \rho(\mathbf{A})} \geq \varepsilon_1 v_i, \quad 1 \leq i \leq N,$$

which implies  $\mathbf{H}(\varepsilon_1 \mathbf{v}) \geq \varepsilon_1 \mathbf{v}$ . And

$$h_i(\varepsilon_2 \mathbf{v}) = \frac{\beta \varepsilon_2 \sum_j a_{ij} v_j}{\gamma_3 + \beta \varepsilon_2 \sum_j a_{ij} v_j} = \frac{\beta \varepsilon_2 v_i \rho(\mathbf{A})}{\gamma_3 + \beta \varepsilon_2 v_i \rho(\mathbf{A})} \leq \varepsilon_2 v_i, \quad 1 \leq i \leq N,$$

which implies  $\mathbf{H}(\varepsilon_2 \mathbf{v}) \leq \varepsilon_2 \mathbf{v}$ . It follows from Claim 1 that  $\mathbf{H}|_K$ , the restriction of  $\mathbf{H}$  on the compact convex set

$$K = [\varepsilon_1 v_1, \varepsilon_2 v_1] \times [\varepsilon_1 v_2, \varepsilon_2 v_2] \times \dots \times [\varepsilon_1 v_N, \varepsilon_2 v_N],$$

maps  $K$  into  $K$ . It follows from the Brouwer Fixed Point Theorem [35] that  $\mathbf{H}$  has a fixed point  $\mathbf{I}^* = (I_1^*, \dots, I_N^*)^T$  in  $K$ .

Next, let us show that  $\mathbf{I}^*$  is the unique fixed point of  $\mathbf{H}$  in  $(0, 1)^N$ . On the contrary, suppose  $\mathbf{H}$  has another fixed point  $\mathbf{J}^* = (J_1^*, \dots, J_N^*)^T$  in  $(0, 1)^N$ . Let

$$\omega = \max_i \frac{I_i^*}{J_i^*}, \quad i_0 = \arg \max_i \frac{I_i^*}{J_i^*}.$$

Without loss of generality, we may assume  $\omega > 1$ , it follows that

$$I_{i_0}^* = h_{i_0}(\mathbf{I}^*) \leq h_{i_0}(\omega \mathbf{J}^*) = \frac{\beta \omega \sum_j a_{i_0 j} J_j^*}{\gamma_3 + \beta \omega \sum_j a_{i_0 j} J_j^*} < \omega \frac{\beta \sum_j a_{i_0 j} J_j^*}{\gamma_3 + \beta \sum_j a_{i_0 j} J_j^*} = \omega h_{i_0}(\mathbf{J}^*) = \omega J_{i_0}^*,$$

which contradicts the assumption that  $I_{i_0}^* = \omega J_{i_0}^*$ . Hence, the fixed point is unique. Claim (a) is proven.

(b) The argument is analogous to that for Claim (a) and hence is omitted.

(c) Suppose that model (2) admits a mixed equilibrium  $\mathbf{E} = (I_1, \dots, I_N, P_1, \dots, P_N)^T$ . By an argument analogous to that for Claim (b), we get that  $P_i = P_i^*$ ,  $1 \leq i \leq N$ . It follows from the first  $N$  equations of model (2) that

$$I_i = \frac{\beta(1 - P_i^*) \sum_j a_{ij} J_j}{\gamma_3 + \beta \sum_j a_{ij} J_j + \gamma_1 \sum_j b_{ij} P_j^*}, \quad 1 \leq i \leq N.$$

The subsequent argument is analogous to that for Claim (a). □

### 3.2. Asymptotic stability of the equilibria

The second step to study the dynamics of model (2) is to examine the asymptotic stability of its equilibria. First, the following lemma gives a criterion for the asymptotic stability of the susceptible equilibrium.

**Lemma 2.** Consider model (2). The following claims hold true.

- (a)  $\mathbf{E}_s$  is asymptotically stable if  $\rho(\mathbf{A}) < \frac{\gamma_3}{\beta}$  and  $\rho(\mathbf{B}) < \frac{\alpha}{\gamma_1}$ .
- (b)  $\mathbf{E}_s$  is a saddle point if  $\rho(\mathbf{A}) > \frac{\gamma_3}{\beta}$  or  $\rho(\mathbf{B}) > \frac{\alpha}{\gamma_1}$ .

**Proof.** The characteristic equation for the Jacobian of model (2) evaluated at  $\mathbf{E}_s$  is

$$\det \begin{pmatrix} \beta \mathbf{A} - (\eta + \gamma_3) \mathbf{E}_N & \mathbf{0} \\ \mathbf{0} & \gamma_1 \mathbf{B} - (\alpha + \eta) \mathbf{E}_N \end{pmatrix} = \det[\beta \mathbf{A} - (\eta + \gamma_3) \mathbf{E}_N] \cdot \det[\gamma_1 \mathbf{B} - (\alpha + \eta) \mathbf{E}_N] = 0.$$

Hereafter  $\mathbf{E}_N$  denotes the identity matrix of order  $N$ .

(a) As  $\beta \mathbf{A} - \gamma_3 \mathbf{E}_N$  and  $\gamma_1 \mathbf{B} - \alpha \mathbf{E}_N$  both have negative spectrum, the roots of the above equation are all negative. The claim follows from the Lyapunov Stability Theorem [36].

(b) Observe that the above equation has a positive root. The claim follows from the Lyapunov Stability Theorem [36].  $\square$

For the purpose of giving criteria for the asymptotic stability of the other three equilibria of model (2), let us define three matrices and present a lemma as follows.

$$\begin{aligned} \mathbf{M}_1 &= \beta \cdot \text{diag}(1 - I_i^*) \cdot \mathbf{A} - \text{diag}\left(\frac{\gamma_3}{1 - I_i^*}\right), \\ \mathbf{M}_2 &= \gamma_1 \cdot \text{diag}(1 - P_i^*) \cdot \mathbf{B} - \text{diag}\left(\frac{\alpha}{1 - P_i^*}\right), \\ \mathbf{M}_3 &= \beta \cdot \text{diag}(1 - I_i^{**} - P_i^*) \cdot \mathbf{A} - \text{diag}\left(\frac{1 - P_i^*}{1 - I_i^{**} - P_i^*} \left[ \gamma_3 + \gamma_1 \sum_j b_{ij} P_j^* \right]\right). \end{aligned}$$

**Lemma 3.** Consider model (2). The following claims hold true.

- (a)  $\mathbf{M}_1$  has a negative spectrum if  $\rho(\mathbf{A}) > \frac{\gamma_3}{\beta}$ .
- (b)  $\mathbf{M}_2$  has a negative spectrum if  $\rho(\mathbf{B}) > \frac{\alpha}{\gamma_1}$ .
- (c) Suppose  $\gamma_1 = \gamma_2$ .  $\mathbf{M}_3$  has a negative spectrum if  $\rho(\mathbf{B}) > \frac{\alpha}{\gamma_1}$  and  $\rho(\mathbf{A}) > \max_i \left\{ \frac{\alpha P_i^* + \gamma_3 (1 - P_i^*)}{\beta (1 - P_i^*)^2} \right\}$ .

The proof of this lemma is left to Appendix A.

**Remark 1.** A common patch-forwarding strategy is to allow a patched node to forward the patches to all of its  $G_p$ -neighbors, without checking their current state. In such situations, the assumption of  $\gamma_1 = \gamma_2$  is rational.

We are ready to give criteria for the asymptotic stability of the other three equilibria of model (2).

**Lemma 4.** Consider model (2). The following claims hold true.

- (a)  $\mathbf{E}_i$  is asymptotically stable if  $\rho(\mathbf{A}) > \frac{\gamma_3}{\beta}$  and  $\rho(\mathbf{B}) < \min\left(\frac{\alpha}{\gamma_1}, \frac{\alpha}{\gamma_2}\right)$ .
- (b)  $\mathbf{E}_p$  is asymptotically stable if  $\rho(\mathbf{A}) < \frac{\gamma_3}{\beta}$  and  $\rho(\mathbf{B}) > \frac{\alpha}{\gamma_1}$ .
- (c) Suppose  $\gamma_1 = \gamma_2$ .  $\mathbf{E}_m$  is asymptotically stable if  $\rho(\mathbf{B}) > \frac{\alpha}{\gamma_1}$  and  $\rho(\mathbf{A}) > \max_i \left\{ \frac{\alpha P_i^* + \gamma_3 (1 - P_i^*)}{\beta (1 - P_i^*)^2} \right\}$ .

**Proof.** (a) Define a matrix as follows.

$$\mathbf{J}_1 = [\gamma_1 \cdot \text{diag}(1 - I_i^*) + \gamma_2 \cdot \text{diag}(I_i^*)] \mathbf{B} - \alpha \mathbf{E}_N.$$

The characteristic equation for the Jacobian of model (2) evaluated at  $\mathbf{E}_i$  is

$$\det \begin{bmatrix} \mathbf{M}_1 - \eta \mathbf{E}_N & \mathbf{0} \\ \mathbf{0} & \mathbf{J}_1 - \eta \mathbf{E}_N \end{bmatrix} = \det(\mathbf{M}_1 - \eta \mathbf{E}_N) \cdot \det(\mathbf{J}_1 - \eta \mathbf{E}_N) = 0.$$

As  $\rho(\mathbf{B}) < \min\left(\frac{\alpha}{\gamma_1}, \frac{\alpha}{\gamma_2}\right) < \min_i \left\{ \frac{\alpha}{\gamma_1 (1 - I_i^*) + \gamma_2 I_i^*} \right\}$ , it follows that  $\mathbf{J}_1$  is Hurwitz. The claim follows from Lemma 3(a) and the Lyapunov Stability Theorem [36].

(b) Define a matrix as follows.

$$\mathbf{J}_2 = \beta \cdot \text{diag}(1 - P_i^*) \cdot \mathbf{A} - \gamma_3 \mathbf{E}_N - \frac{\alpha \gamma_2}{\gamma_1} \text{diag}\left(\frac{P_i^*}{1 - P_i^*}\right).$$

The characteristic equation for the Jacobian of model (2) evaluated at  $\mathbf{E}_p$  is

$$\det \begin{bmatrix} \mathbf{J}_2 - \eta \mathbf{E}_N & \mathbf{0} \\ \mathbf{0} & \mathbf{M}_2 - \eta \mathbf{E}_N \end{bmatrix} = \det(\mathbf{J}_2 - \eta \mathbf{E}_N) \cdot \det(\mathbf{M}_2 - \eta \mathbf{E}_N) = 0.$$

As  $\rho(\mathbf{A}) < \frac{\gamma_3}{\beta} < \min_i \left\{ \frac{\alpha \gamma_2 P_i^* + \gamma_1 \gamma_3 (1 - P_i^*)}{\beta \gamma_1 (1 - P_i^*)^2} \right\}$ , it follows that  $\mathbf{J}_2$  is Hurwitz. The claim follows from Lemma 3(b) and the Lyapunov Stability Theorem [36].

(c) The characteristic equation for the Jacobian of model (2) evaluated at  $\mathbf{E}_m$  is

$$\det \begin{bmatrix} \mathbf{M}_3 - \eta \mathbf{E}_N & \mathbf{0} \\ \mathbf{0} & \mathbf{M}_2 - \eta \mathbf{E}_N \end{bmatrix} = \det(\mathbf{M}_3 - \eta \mathbf{E}_N) \cdot \det(\mathbf{M}_2 - \eta \mathbf{E}_N) = 0.$$

Hence, the claim follows from Lemma 3(a) and (b) as well as the Lyapunov Stability Theorem [36].  $\square$

3.3. Global stability of the equilibria

The third step to study the dynamics of model (2) is to examine the global stability of its equilibria. The following theorem gives criteria for the global stability of the four equilibria of model (2).

**Theorem 2.** Consider model (2).

- (a) If  $\rho(\mathbf{A}) < \frac{\gamma_3}{\beta}$  and  $\rho(\mathbf{B}) < \frac{\alpha}{\gamma_1}$ , then  $\mathbf{E}_S$  is asymptotically stable with respect to  $\Omega$ .
- (b) If  $\rho(\mathbf{A}) > \frac{\gamma_3}{\beta}$  and  $\rho(\mathbf{B}) < \min\{\frac{\alpha}{\gamma_1}, \frac{\alpha}{\gamma_2}\}$ , then  $\mathbf{E}_i$  is asymptotically stable with respect to  $\{(\mathbf{I}, \mathbf{P}) \in \Omega: \mathbf{I} \neq \mathbf{0}\}$ .
- (c) If  $\rho(\mathbf{A}) < \frac{\gamma_3}{\beta}$  and  $\rho(\mathbf{B}) > \frac{\alpha}{\gamma_1}$ , then  $\mathbf{E}_p$  is asymptotically stable with respect to  $\{(\mathbf{I}, \mathbf{P}) \in \Omega: \mathbf{P} \neq \mathbf{0}\}$ .
- (d) Suppose  $\gamma_1 = \gamma_2$ . If  $\rho(\mathbf{B}) > \frac{\alpha}{\gamma_1}$  and  $\rho(\mathbf{A}) > \max_i\{\frac{\alpha P_i^* + \gamma_3(1-P_i^*)}{\beta(1-P_i^*)^2}\}$ , then  $\mathbf{E}_m$  is asymptotically stable with respect to  $\{(\mathbf{I}, \mathbf{P}) \in \Omega: \mathbf{I} \neq \mathbf{0}, \mathbf{P} \neq \mathbf{0}\}$ .

**Proof.** Let  $(I_1(t), \dots, I_N(t), P_1(t), \dots, P_N(t))^T$  be a solution to model (2), and let

$$\mathbf{I}(t) = (I_1(t), \dots, I_N(t))^T, \quad \mathbf{P}(t) = (P_1(t), \dots, P_N(t))^T.$$

(a) It follows from the first  $N$  equations of model (2) that

$$\frac{d\mathbf{I}(t)}{dt} \leq -\gamma_3\mathbf{I}(t) + \beta\mathbf{A}\mathbf{I}(t).$$

Consider the comparison system

$$\frac{d\mathbf{u}(t)}{dt} = -\gamma_3\mathbf{u}(t) + \beta\mathbf{A}\mathbf{u}(t), \quad \mathbf{u}(0) = \mathbf{I}(0). \tag{4}$$

Define a positive definite function as  $V_1(\mathbf{u}) = \frac{1}{2}\mathbf{u}^T\mathbf{u}$ . By calculation, we get that

$$\frac{dV_1(\mathbf{u}(t))}{dt} |_{(4)} = \mathbf{u}^T[\beta\mathbf{A} - \gamma_3\mathbf{E}_N]\mathbf{u}(t) \leq 0.$$

Moreover,  $\frac{dV_1(\mathbf{u}(t))}{dt} |_{(4)} = 0$  if and only if  $\mathbf{u}(t) = \mathbf{0}$ . It follows by the LaSalle Invariance Principle [36] that  $\mathbf{u}(t) \rightarrow \mathbf{0}$ . According to the comparison theorem for higher-dimensional dynamical systems [36], we get that  $\mathbf{I}(t) \leq \mathbf{u}(t)$ , implying that  $\mathbf{I}(t) \rightarrow \mathbf{0}$ . Thus, model (2) can be reduced to the following limiting system [37].

$$\frac{d\mathbf{v}(t)}{dt} = -\alpha\mathbf{v}(t) + \text{diag}(1 - v_i(t)) \cdot \gamma_1\mathbf{B}\mathbf{v}(t). \tag{5}$$

Likewise, we can deduce that  $\mathbf{v}(t) \rightarrow \mathbf{0}$ , implying  $\mathbf{P}(t) \rightarrow \mathbf{0}$ . Therefore, the claim follows from Lemma 2(a).

(b) Suppose that  $\mathbf{I}(0) \neq \mathbf{0}$ . It follows from the last  $N$  equations of model (2) that

$$\frac{d\mathbf{P}(t)}{dt} \leq -\alpha\mathbf{P}(t) + \max\{\gamma_1, \gamma_2\}\mathbf{B}\mathbf{P}(t).$$

Similar to the argument for Claim (a), we get  $\mathbf{P}(t) \rightarrow \mathbf{0}$ . Thus, model (2) can be reduced to the following limiting system.

$$\frac{d\mathbf{w}(t)}{dt} = -\gamma_3\mathbf{w}(t) + \text{diag}(1 - w_i(t)) \cdot \beta\mathbf{A}\mathbf{w}(t). \tag{6}$$

Theorem 1 ensures that the system admits a unique nonzero equilibrium  $\mathbf{I}^*$ . Let  $\mathbf{y}(t) = \mathbf{w}(t) - \mathbf{I}^*$ , and rewrite system (6) as

$$\frac{d\mathbf{y}(t)}{dt} = -\gamma_3\mathbf{y}(t) + \text{diag}(1 - y_i(t) - I_i^*) \cdot \beta\mathbf{A}\mathbf{y}(t) - \text{diag}(y_i(t)) \cdot \beta\mathbf{A}\mathbf{I}^*. \tag{7}$$

Define a positive definite function as

$$V_2(\mathbf{y}) = \frac{1}{2}\mathbf{y}^T \cdot \text{diag}\left(\frac{1}{1 - I_i^*}\right) \cdot \mathbf{y}.$$

By calculation, we get that

$$\begin{aligned} \frac{dV_2(\mathbf{y}(t))}{dt} |_{(7)} &= \mathbf{y}(t)^T \mathbf{C}_3\mathbf{y}(t) - \beta\mathbf{y}(t)^T \cdot \text{diag}\left(\frac{y_i(t)}{1 - I_i^*}\right) \cdot \mathbf{A}\mathbf{y}(t) \\ &= \mathbf{y}(t)^T \mathbf{C}_1\mathbf{y}(t) - \beta\mathbf{y}(t)^T \cdot \text{diag}\left(\frac{y_i(t)}{1 - I_i^*}\right) \cdot \mathbf{A}(\mathbf{y}(t) + \mathbf{I}^*) \leq 0. \end{aligned}$$

Moreover, it is easily verified that the union of complete trajectories contained entirely in the set  $\{\mathbf{y}(t) : \frac{dV_2(\mathbf{y}(t))}{dt} |_{(7)} = 0\}$  contains no nontrivial trajectory of system (7). According to the LaSalle Invariance Principle [36], we have  $\mathbf{y}(t) \rightarrow \mathbf{0}$ , implying  $\mathbf{I}(t) \rightarrow \mathbf{I}^*$ . Hence, the claim follows from Claim (a) of Lemma 4.

(c) The argument is analogous to that for Claim (b) and hence is omitted.

(d) Suppose that  $\mathbf{I}(0) \neq \mathbf{0}$  and  $\mathbf{P}(0) \neq \mathbf{0}$ . As  $\gamma_1 = \gamma_2$ , the last  $N$  equations of model (2) reduce to

$$\frac{d\mathbf{P}(t)}{dt} = -\alpha\mathbf{P}(t) + \text{diag}(1 - P_i(t)) \cdot \gamma_1\mathbf{B}\mathbf{P}(t), \quad i = 1, 2, \dots, N.$$

Similar to the argument for Claim (c), we get  $\mathbf{P}(t) \rightarrow \mathbf{P}^*$ . So, model (2) can be reduced to the following limiting system.

$$\frac{d\mathbf{z}(t)}{dt} = -\gamma_3\mathbf{z}(t) + \text{diag}(1 - z_i(t) - P_i^*) \cdot \beta\mathbf{A}\mathbf{z}(t) - \text{diag}(z_i(t)) \cdot \gamma_1\mathbf{B}\mathbf{P}^*. \tag{8}$$

Let  $\mathbf{p}(t) = \mathbf{z}(t) - \mathbf{I}^{**}$ , and rewrite system (8) as

$$\frac{d\mathbf{p}(t)}{dt} = -\gamma_3\mathbf{p}(t) + \text{diag}(1 - p_i(t) - I_i^{**} - P_i^*) \cdot \beta\mathbf{A}\mathbf{p}(t) - \beta \cdot \text{diag}(p_i(t)) \cdot \mathbf{A}\mathbf{I}^{**} - \text{diag}(p_i(t)) \cdot \gamma_1\mathbf{B}\mathbf{P}^*. \tag{9}$$

Define a positive definite function as

$$V_3(\mathbf{p}) = \frac{1}{2}\mathbf{p}^T \cdot \text{diag}\left(\frac{1}{1 - I_i^{**} - P_i^*}\right) \cdot \mathbf{p}.$$

By calculation, we get

$$\begin{aligned} \frac{dV_3(\mathbf{p}(t))}{dt} \Big|_{(9)} &= \mathbf{p}(t)^T \mathbf{G}_3\mathbf{p}(t) - \beta\mathbf{p}(t)^T \cdot \text{diag}\left(\frac{p_i(t)}{1 - I_i^{**} - P_i^*}\right) \cdot \mathbf{A}\mathbf{p}(t) \\ &= \mathbf{p}(t)^T \mathbf{G}_1\mathbf{p}(t) - \beta\mathbf{p}(t)^T \cdot \text{diag}\left(\frac{p_i(t)}{1 - I_i^{**} - P_i^*}\right) \cdot \mathbf{A}(\mathbf{p}(t) + \mathbf{I}^{**}) \leq 0. \end{aligned}$$

Moreover, it is easily verified that the union of complete trajectories contained entirely in the set  $\{\mathbf{z}(t) : \frac{dV_2(\mathbf{p}(t))}{dt} \Big|_{(9)} = 0\}$  contains no nontrivial trajectory of system (9). According to the LaSalle Invariance Principle [36], we get  $\mathbf{p}(t) \rightarrow \mathbf{0}$ , implying  $\mathbf{I}(t) \rightarrow \mathbf{I}^{**}$ . Hence, the claim follows from Lemma 4(c). □

Let  $I(t)$  denote the expected fraction of infected nodes at time  $t$ , and let  $P(t)$  denote the expected fraction of patched nodes at time  $t$ . That is,

$$I(t) = \frac{1}{N} \sum_{i=1}^N I_i(t), \quad P(t) = \frac{1}{N} \sum_{i=1}^N P_i(t).$$

One major concern of malware epidemic dynamics is to understand the evolving tendency of  $I(t)$  and  $P(t)$  over time. For that purpose, let

$$I^* = \frac{1}{N} \sum_{i=1}^N I_i^*, \quad I^{**} = \frac{1}{N} \sum_{i=1}^N I_i^{**}, \quad P^* = \frac{1}{N} \sum_{i=1}^N P_i^*.$$

As a direct consequence of Theorem 2, the following theorem helps decide on this tendency.

**Theorem 3.** Consider model (2). The following claims hold.

- (a) If  $\rho(\mathbf{A}) < \frac{\gamma_3}{\beta}$  and  $\rho(\mathbf{B}) < \frac{\alpha}{\gamma_1}$ , then  $I(t) \rightarrow 0, P(t) \rightarrow 0$ .
- (b) If  $\rho(\mathbf{A}) > \frac{\gamma_3}{\beta}$  and  $\rho(\mathbf{B}) < \min\{\frac{\alpha}{\gamma_1}, \frac{\alpha}{\gamma_2}\}$ ,  $I(0) \neq 0$ , then  $I(t) \rightarrow I^*, P(t) \rightarrow 0$ .
- (c) If  $\rho(\mathbf{A}) < \frac{\gamma_3}{\beta}$  and  $\rho(\mathbf{B}) > \frac{\alpha}{\gamma_1}$ ,  $P(0) \neq 0$ , then  $I(t) \rightarrow 0, P(t) \rightarrow P^*$ .
- (d) Suppose  $\gamma_1 = \gamma_2$ . If  $\rho(\mathbf{B}) > \frac{\alpha}{\gamma_1}$  and  $\rho(\mathbf{A}) > \max_i\{\frac{\alpha P_i^* + \gamma_3(1 - P_i^*)}{\beta(1 - P_i^*)^2}\}$ ,  $I(0) \neq 0, P(0) \neq 0$ , then  $I(t) \rightarrow I^{**}, P(t) \rightarrow P^*$ .

### 4. Numerical examples

In this section, let us give some numerical examples of model (2).

#### 4.1. Scale-free virus-spreading network vs. scale-free patch-forwarding network

It is well known that many real-world networks are scale-free, i.e., their degree distributions approximately follow a power law [38]. The method proposed by Barabasi and Albert [38] can be used to generate scale-free networks.

**Example 1.** Generate a scale-free network with 300 nodes using the Barabasi–Albert method. Take this network as the patch-forwarding network  $G_p$  as well as the virus-spreading network  $G_v$ . Numerical calculations give  $\lambda_{\max}(\mathbf{A}) = \lambda_{\max}(\mathbf{B}) = 4.3602$ .

- (a) Suppose  $\alpha = 0.1, \beta = 0.02, \gamma_1 = 0.01, \gamma_2 = 0.015, \gamma_3 = 0.2$ . As  $\lambda_{\max}(\mathbf{A}) < \min\{\frac{\gamma_3}{\beta}, \frac{\alpha}{\gamma_1}\}$ , it follows from Theorem 3(a) that  $I(t) \rightarrow 0$  and  $P(t) \rightarrow 0$ . Fig. 2a shows the time plots of  $I(t)$  (red lines) and  $P(t)$  (green lines) under four different initial conditions.

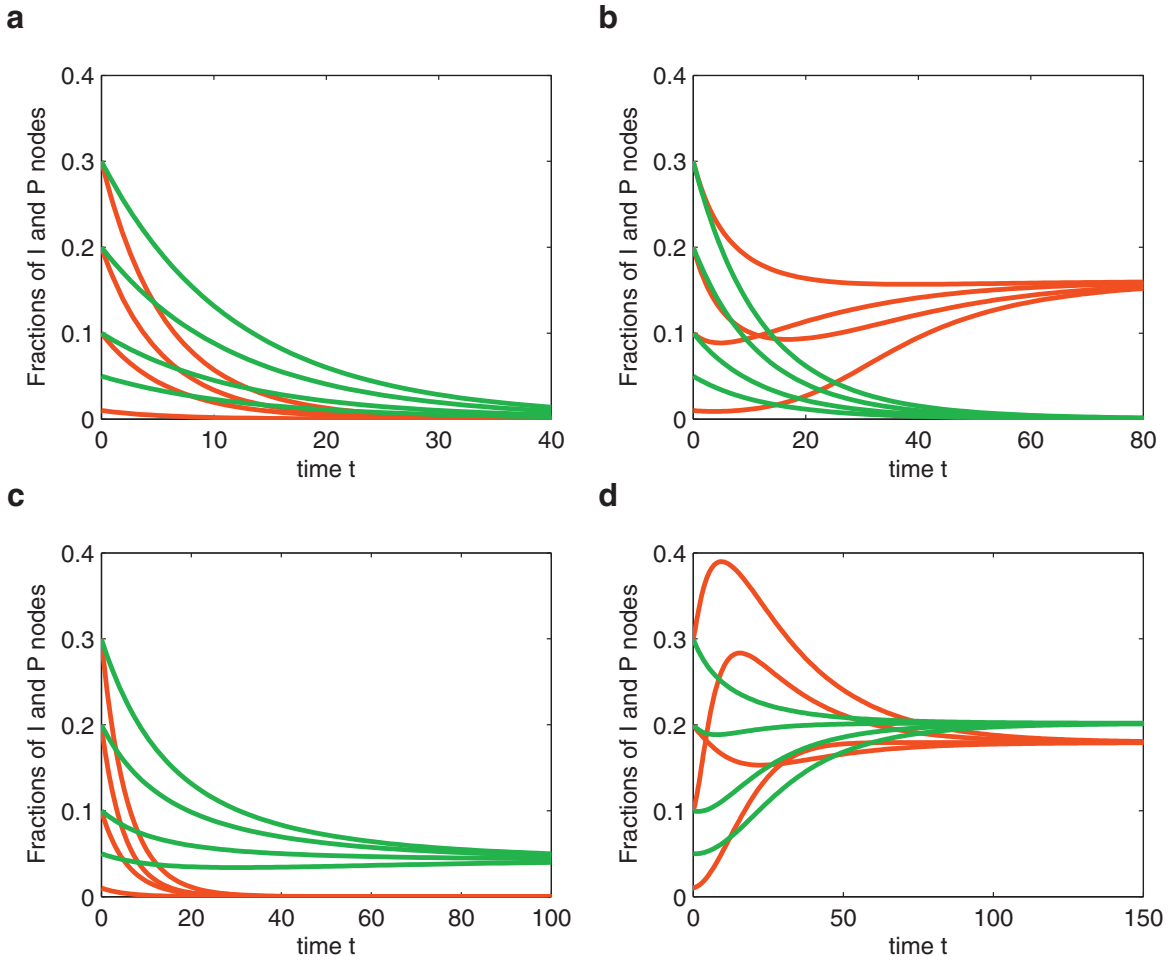


**Fig. 2.** The time plots of  $I(t)$  and  $P(t)$  for [Example 1](#). (For interpretation of the references to color in this figure, the reader is referred to the web version of this article.)

- (b) Suppose  $\alpha = 0.1$ ,  $\beta = 0.06$ ,  $\gamma_1 = 0.01$ ,  $\gamma_2 = 0.15$ ,  $\gamma_3 = 0.2$ . As  $\frac{\gamma_3}{\beta} < \lambda_{\max}(\mathbf{A}) < \min\{\frac{\alpha}{\gamma_1}, \frac{\alpha}{\gamma_2}\}$ , it follows from [Theorem 3\(b\)](#) that  $I(t) \rightarrow I^*$  and  $P(t) \rightarrow 0$  if  $I(0) \neq 0$ . [Fig. 2b](#) exhibits the time plots of  $I(t)$  (red lines) and  $P(t)$  (green lines) under four different initial conditions, according with the prediction.
- (c) Suppose  $\alpha = 0.1$ ,  $\beta = 0.02$ ,  $\gamma_1 = 0.03$ ,  $\gamma_2 = 0.04$ ,  $\gamma_3 = 0.2$ . As  $\frac{\alpha}{\gamma_1} < \lambda_{\max}(\mathbf{A}) < \frac{\gamma_3}{\beta}$ , it follows from [Theorem 3\(c\)](#) that  $I(t) \rightarrow 0$  and  $P(t) \rightarrow P^*$  if  $P(0) \neq 0$ . [Fig. 2c](#) shows the time plots of  $I(t)$  (red lines) and  $P(t)$  (green lines) under four different initial conditions.
- (d) Suppose  $\alpha = 0.1$ ,  $\beta = 0.2$ ,  $\gamma_1 = \gamma_2 = 0.05$ ,  $\gamma_3 = 0.2$ . As  $\lambda_{\max}(\mathbf{A}) > \frac{\alpha}{\gamma_1}$  and  $\lambda_{\max}(\mathbf{A}) > \max_i\{\frac{\alpha P_i^* + \gamma_3(1-P_i^*)}{\beta(1-P_i^*)^2}\}$ , it follows from [Theorem 2\(d\)](#) that  $I(t) \rightarrow I^{**}$  and  $P(t) \rightarrow P^*$  if  $I(0) \neq 0$  and  $P(0) \neq 0$ . [Fig. 2d](#) displays the time plots of  $I(t)$  (red lines) and  $P(t)$  (green lines) under four different initial conditions.

**4.2. Scale-free virus-spreading network vs. small-world patch-forwarding network**

It is well known that many real-world networks are small-world, i.e., they have a short characteristic path length as well as a high clustering coefficient [39]. The method proposed by Watts and Strogatz [39] can be used to generate small-world networks.

**Example 2.** Generate a small-world network with 300 nodes using the Watts–Strogatz method. Take this network as the patch-forwarding network  $G_p$ . Numerical calculations give  $\lambda_{\max}(\mathbf{B}) = 10.4250$ . In addition, take the scale-free network in [Example 1](#) as the virus-spreading network  $G_v$ . Hence,  $\lambda_{\max}(\mathbf{A}) = 4.3602$ .

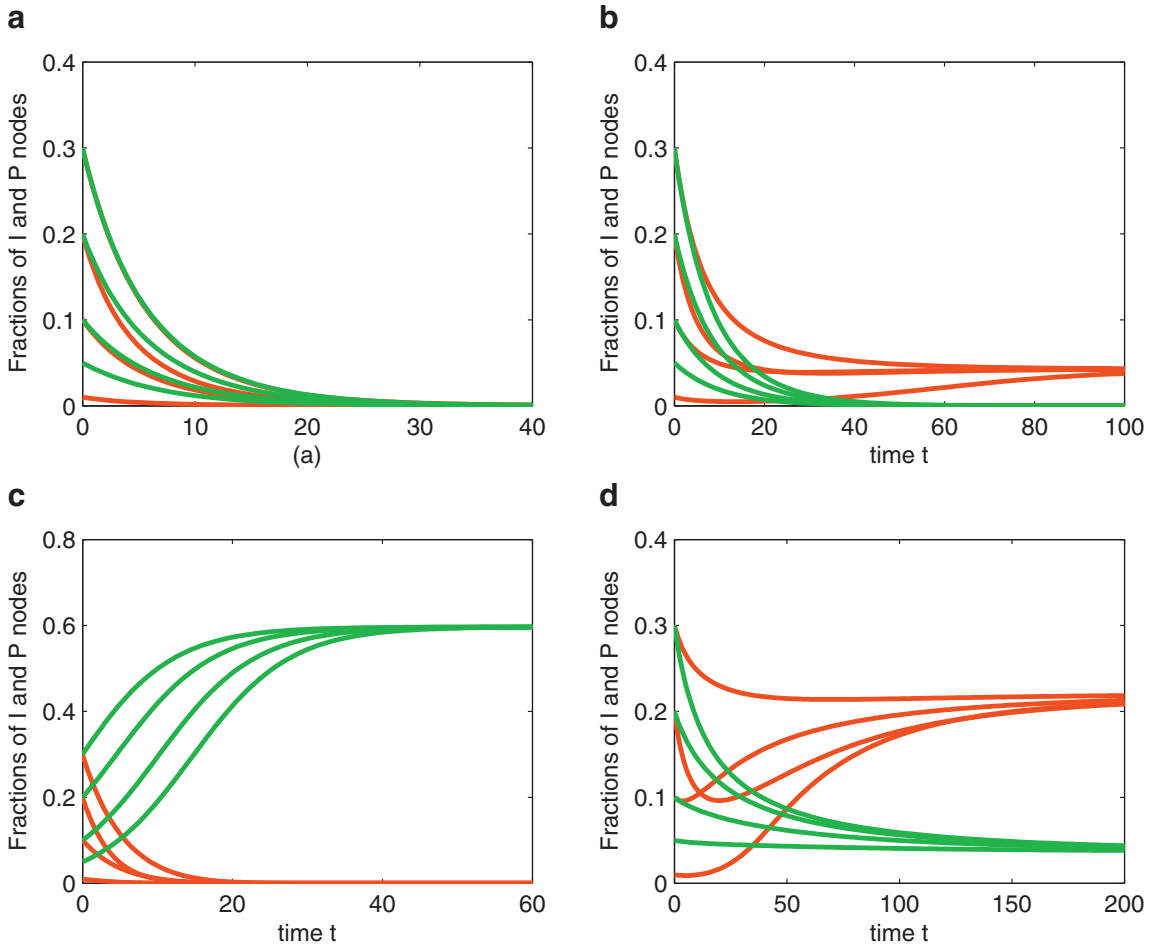


**Fig. 3.** The time plots of  $I(t)$  and  $P(t)$  for Example 2. (For interpretation of the references to color in this figure, the reader is referred to the web version of this article.)

- (a) Suppose  $\alpha = 0.3$ ,  $\beta = 0.02$ ,  $\gamma_1 = 0.015$ ,  $\gamma_2 = 0.02$ ,  $\gamma_3 = 0.2$ . As  $\lambda_{\max}(\mathbf{A}) < \frac{\gamma_3}{\beta}$  and  $\lambda_{\max}(\mathbf{B}) < \frac{\alpha}{\gamma_1}$ , it follows from Theorem 3(a) that  $I(t) \rightarrow 0$  and  $P(t) \rightarrow 0$ . Fig. 3a shows the time plots of  $I(t)$  (red lines) and  $P(t)$  (green lines) under four different initial conditions.
- (b) Suppose  $\alpha = 0.2$ ,  $\beta = 0.06$ ,  $\gamma_1 = 0.01$ ,  $\gamma_2 = 0.012$ ,  $\gamma_3 = 0.2$ . As  $\lambda_{\max}(\mathbf{A}) > \frac{\gamma_3}{\beta}$  and  $\lambda_{\max}(\mathbf{B}) < \min\{\frac{\alpha}{\gamma_1}, \frac{\alpha}{\gamma_1}\}$ , it follows from Theorem 3(b) that  $I(t) \rightarrow I^*$  and  $P(t) \rightarrow 0$  if  $I(0) \neq 0$ . Fig. 3b exhibits the time plots of  $I(t)$  (red lines) and  $P(t)$  (green lines) under four different initial conditions.
- (c) Suppose  $\alpha = 0.1$ ,  $\beta = 0.02$ ,  $\gamma_1 = 0.025$ ,  $\gamma_2 = 0.03$ ,  $\gamma_3 = 0.2$ . As  $\lambda_{\max}(\mathbf{A}) < \frac{\gamma_3}{\beta}$  and  $\lambda_{\max}(\mathbf{B}) > \frac{\alpha}{\gamma_1}$ , it follows from Theorem 3(c) that  $I(t) \rightarrow 0$  and  $P(t) \rightarrow P^*$  if  $P(0) \neq 0$ . Fig. 3c displays the time plots of  $I(t)$  (red lines) and  $P(t)$  (green lines) under four different initial conditions.
- (d) Suppose  $\alpha = 0.2$ ,  $\beta = 0.06$ ,  $\gamma_1 = 0.02 = \gamma_2 = 0.02$ ,  $\gamma_3 = 0.1$ . As  $\lambda_{\max}(\mathbf{B}) > \frac{\alpha}{\gamma_1}$  and  $\lambda_{\max}(\mathbf{A}) > \max_i\{\frac{\alpha P_i^* + \gamma_3(1-P_i^*)}{\beta(1-P_i^*)^2}\}$ , it follows from Theorem 3(d) that  $I(t) \rightarrow I^{**}$  and  $P(t) \rightarrow P^*$  if  $I(0) \neq 0$  and  $P(0) \neq 0$ . Fig. 3d displays the time plots of  $I(t)$  (red lines) and  $P(t)$  (green lines) under four different initial conditions.

### 4.3. Real-world virus-spreading network vs. real-world patch-forwarding network

The Facebook network given in <http://snap.stanford.edu/data/egonets-Facebook.html>, which consists of 4039 nodes and 88234 edges, is a piece of the whole Facebook network. Computer viruses can propagate through the network, and patches can be disseminated through the same network.

**Example 3.** Take the above mentioned network as the patch-forwarding network  $G_p$  as well as the virus-spreading network  $G_v$ . Numerical calculations give  $\lambda_{\max}(\mathbf{A}) = \lambda_{\max}(\mathbf{B}) = 162.3739$ .

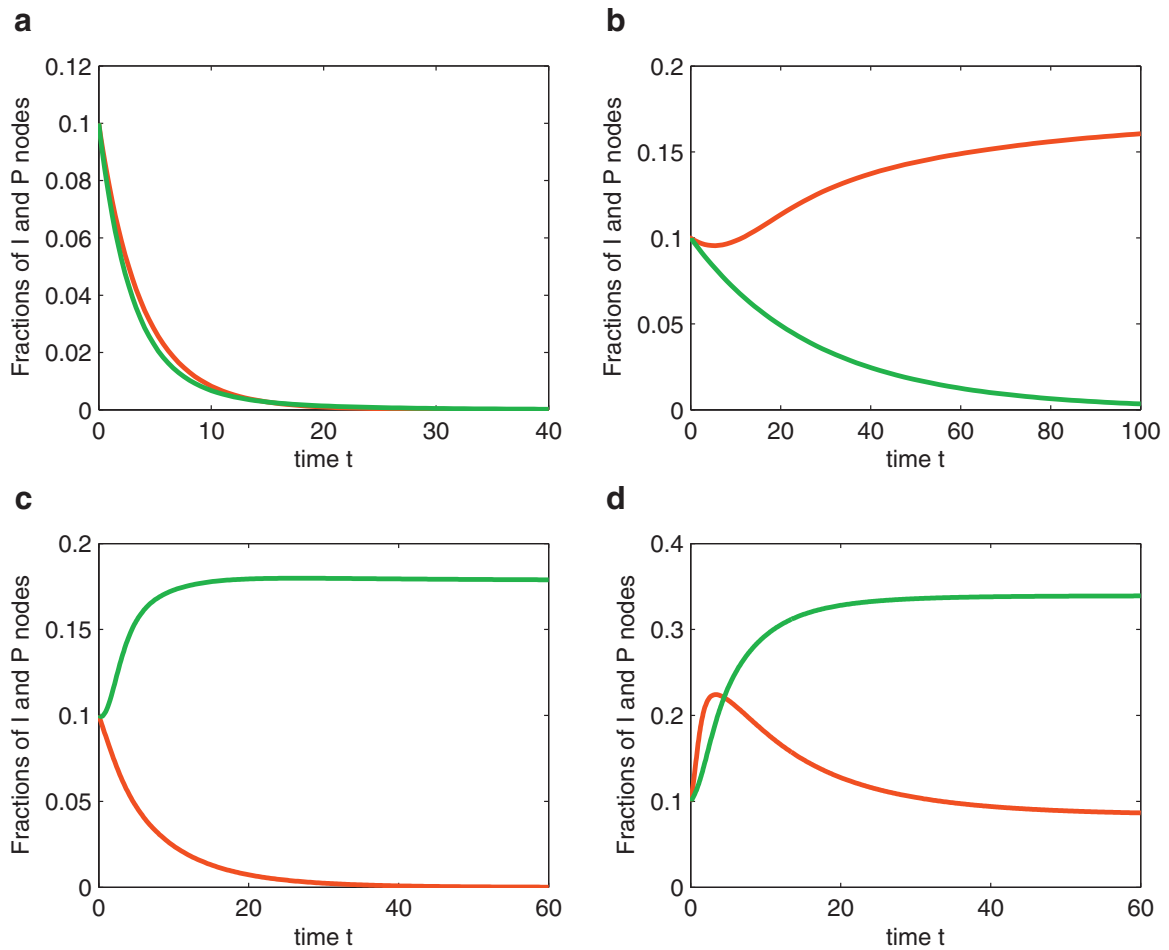


**Fig. 4.** The time plots of  $I(t)$  and  $P(t)$  for Example 3. (For interpretation of the references to color in this figure, the reader is referred to the web version of this article.)

- (a) Suppose  $\alpha = 0.4$ ,  $\beta = 0.001$ ,  $\gamma_1 = 0.002$ ,  $\gamma_2 = 0.00025$ ,  $\gamma_3 = 0.3$ . As  $\lambda_{\max}(\mathbf{A}) < \min\{\frac{\gamma_3}{\beta}, \frac{\alpha}{\gamma_1}\}$ , it follows from Theorem 3(a) that  $I(t) \rightarrow 0$  and  $P(t) \rightarrow 0$ . Fig. 4a shows a time plot of  $I(t)$  (red line) and the corresponding time plot of  $P(t)$  (green line).
- (b) Suppose  $\alpha = 0.04$ ,  $\beta = 0.0015$ ,  $\gamma_1 = 0.0001$ ,  $\gamma_2 = 0.00012$ ,  $\gamma_3 = 0.07$ . As  $\frac{\gamma_3}{\beta} < \lambda_{\max}(\mathbf{A}) < \min\{\frac{\alpha}{\gamma_1}, \frac{\alpha}{\gamma_1}\}$ , it follows from Theorem 3(b) that  $I(t) \rightarrow I^*$  and  $P(t) \rightarrow 0$  if  $I(0) \neq 0$ . Fig. 4b exhibits a time plot of  $I(t)$  (red line) and the corresponding time plot of  $P(t)$  (green line).
- (c) Suppose  $\alpha = 0.4$ ,  $\beta = 0.0003$ ,  $\gamma_1 = 0.009$ ,  $\gamma_2 = 0.009$ ,  $\gamma_3 = 0.1$ . As  $\frac{\alpha}{\gamma_1} < \lambda_{\max}(\mathbf{A}) < \frac{\gamma_3}{\beta}$ , it follows from Theorem 3(c) that  $I(t) \rightarrow 0$  and  $P(t) \rightarrow P^*$  if  $P(0) \neq 0$ . Fig. 4c displays a time plot of  $I(t)$  (red line) and the corresponding time plot of  $P(t)$  (green line).
- (d) Suppose  $\alpha = 0.2$ ,  $\beta = 0.02$ ,  $\gamma_1 = \gamma_2 = 0.008$ ,  $\gamma_3 = 0.2$ . As  $\lambda_{\max}(\mathbf{A}) > \frac{\alpha}{\gamma_1}$  and  $\lambda_{\max}(\mathbf{A}) > \max_i\{\frac{\alpha P_i^* + \gamma_3(1-P_i^*)}{\beta(1-P_i^*)^2}\}$ , it follows from Theorem 3(d) that  $I(t) \rightarrow I^{**}$  and  $P(t) \rightarrow P^*$  if  $I(0) \neq 0$  and  $P(0) \neq 0$ . Fig. 4d displays a time plot of  $I(t)$  (red line) and the corresponding time plot of  $P(t)$  (green line).

**5. Further discussions**

This section addresses the application of Theorem 3 in the containment of the viral prevalence.

**5.1. Eradicating the malware**

Theorem 3 (c) informs that when  $\rho(\mathbf{A}) < \frac{\gamma_3}{\beta}$  and  $\rho(\mathbf{B}) > \frac{\alpha}{\gamma_1}$ , even a single patched node can lead to the eradication of the malware in the network. This shows that if the budget is sufficient, the malware in a network can be wiped out by taking the following measures simultaneously.

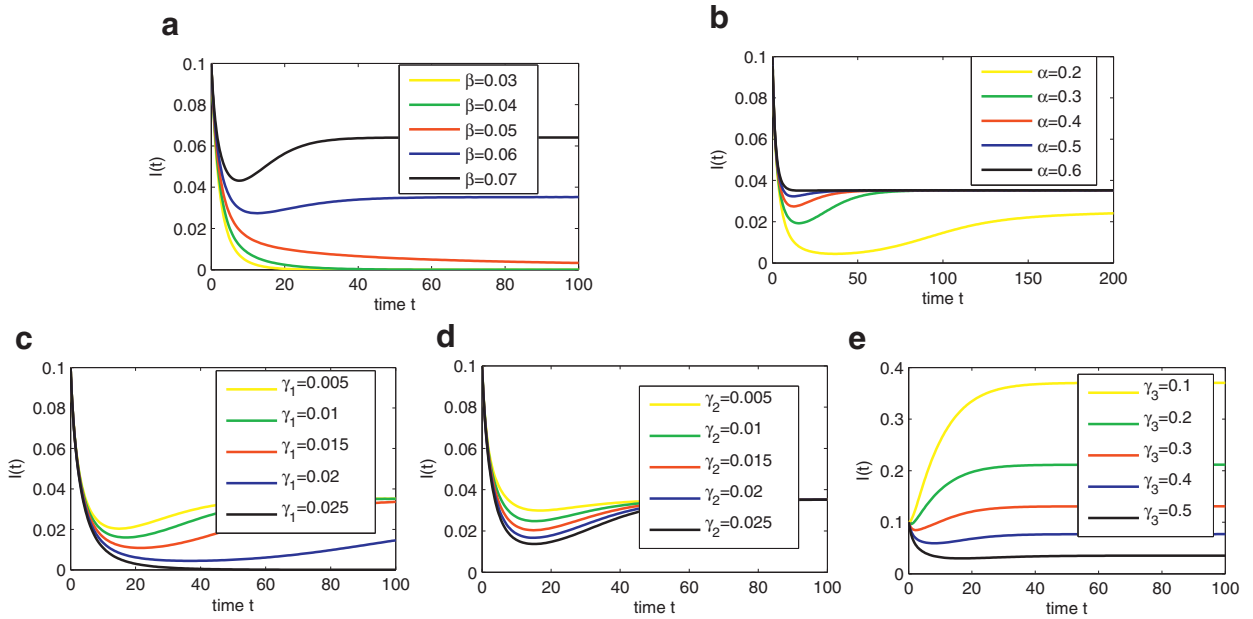


Fig. 5. The time plots of  $I(t)$  for different values of parameters.

- (1) Reduce the spectral radius of the virus-spreading network.
- (2) Enhance the spectral radius of the patch-forwarding network.
- (3) Reduce the values of  $\beta$  and  $\alpha$ .
- (4) Enhance the values of  $\gamma_1$  and  $\gamma_3$ .

**Remark 2.** It is well known from the spectral theory that deleting edges from a network would reduce its spectral radius, whereas adding edges to a network would enhance its spectral radius [34]. Therefore, the routes through which malware spread should be reduced, and the routes through which patches are forwarded should be reduced, so as to wipe out the malware.

### 5.2. Reducing the final expected fraction of the infected nodes

Due to the limited budget in real-world applications, it may be impractical to meet  $\rho(\mathbf{A}) < \frac{\gamma_3}{\beta}$  and  $\rho(\mathbf{B}) > \frac{\alpha}{\gamma_1}$  simultaneously. In such situations, the best thing we can do is to manage to reduce the final expected fraction of infected nodes and to enhance the final expected fraction of patched nodes. A question arises naturally: how can we achieve this goal? To answer this question, we present the following theorem.

**Theorem 4.** Consider model (2). The following claims hold true.

- (a) If  $\rho(\mathbf{A}) > \frac{\gamma_3}{\beta}$ , then  $\frac{\partial I_i^*}{\partial \beta} > 0$ ,  $\frac{\partial I_i^*}{\partial \gamma_3} < 0$ ,  $1 \leq i \leq N$ .
- (b) If  $\rho(\mathbf{B}) > \frac{\alpha}{\gamma_1}$ , then  $\frac{\partial P_i^*}{\partial \gamma_1} > 0$ ,  $\frac{\partial P_i^*}{\partial \alpha} < 0$ ,  $1 \leq i \leq N$ .
- (c) Suppose  $\gamma_1 = \gamma_2$ . If  $\rho(\mathbf{B}) > \frac{\alpha}{\gamma_1}$  and  $\rho(\mathbf{A}) > \max_i \left\{ \frac{\alpha P_i^* + \gamma_3 (1 - P_i^*)}{\beta (1 - P_i^*)^2} \right\}$ , then  $\frac{\partial I_i^{**}}{\partial \beta} > 0$ ,  $\frac{\partial I_i^{**}}{\partial \gamma_1} < 0$ , and  $\frac{\partial I_i^{**}}{\partial \gamma_3} < 0$ ,  $1 \leq i \leq N$ .

The proof of this theorem is left to Appendix B. Figs. 5 and 6 illustrates this theorem.

The following theorem is a direct consequence of Theorem 4.

**Theorem 5.** Consider model (2). The following claims hold true.

- (a) If  $\rho(\mathbf{A}) > \frac{\gamma_3}{\beta}$ , then  $\frac{\partial I_i^*}{\partial \beta} > 0$ ,  $\frac{\partial I_i^*}{\partial \gamma_3} < 0$ .
- (b) If  $\rho(\mathbf{B}) > \frac{\alpha}{\gamma_1}$ , then  $\frac{\partial P_i^*}{\partial \gamma_1} > 0$ ,  $\frac{\partial P_i^*}{\partial \alpha} < 0$ .
- (c) Suppose  $\gamma_1 = \gamma_2$ . If  $\rho(\mathbf{B}) > \frac{\alpha}{\gamma_1}$  and  $\rho(\mathbf{A}) > \max_i \left\{ \frac{\alpha P_i^* + \gamma_3 (1 - P_i^*)}{\beta (1 - P_i^*)^2} \right\}$ , then  $\frac{\partial I_i^{**}}{\partial \beta} > 0$ ,  $\frac{\partial I_i^{**}}{\partial \gamma_1} < 0$ , and  $\frac{\partial I_i^{**}}{\partial \gamma_3} < 0$ .

By this theorem, the following measures should be taken to reduce the asymptotic expected fraction of infected nodes or to enhance the asymptotic expected fraction of patched nodes.

- (1) Reduce the values of  $\beta$  and  $\alpha$ .
- (2) Enhance the values of  $\gamma_1$  and  $\gamma_3$ .

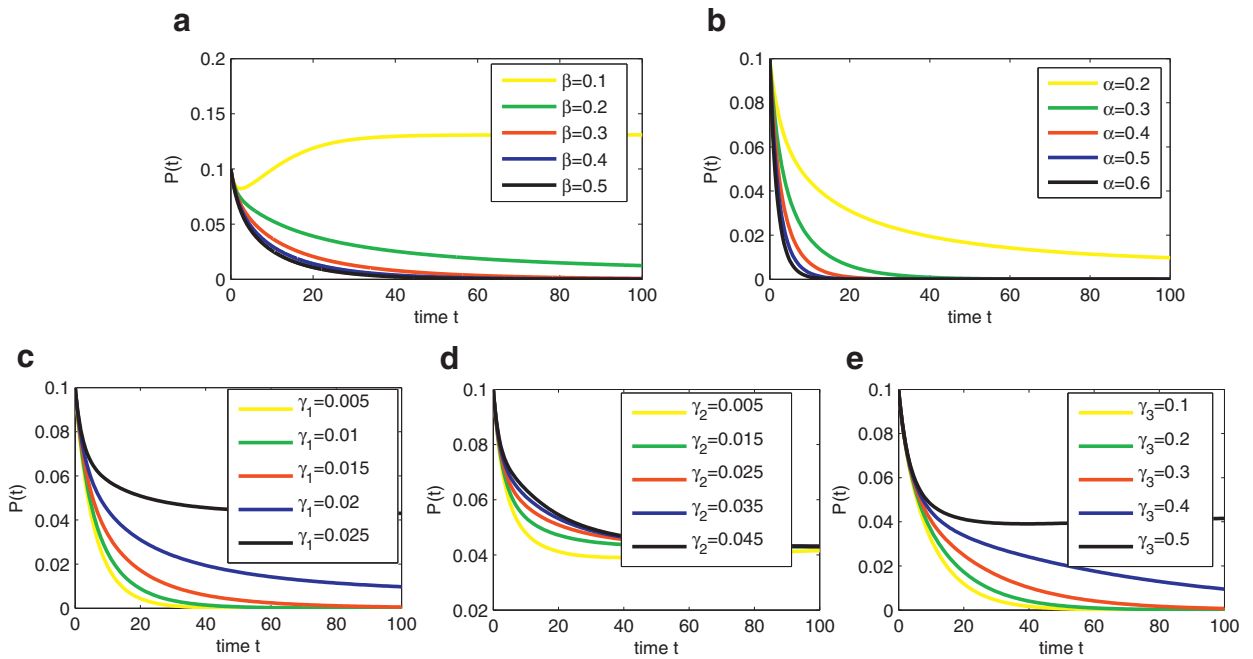


Fig. 6. The time plots of  $P(t)$  for different values of parameters.

### 6. Conclusions and remarks

For the purpose of assessing the impact of patch forwarding on the prevalence of computer virus, a node-level malware propagation model (the node-level SIPS model) has been proposed. It has been found that the spectral radii of the patch-forwarding network and virus-spreading network both have a significant impact on the viral prevalence. Numerical examples based on synthetic and real-world networks have been given to illustrate the theoretical results. The influence of some key factors on the virus prevalence has been revealed. Thereby, some strategies of containing electronic infections are recommended.

Towards this direction, lots of work have yet to be done. First, our work should be extended to the situation that neither of the four conditions in Theorem 3 is met. Second, our model assumes that all nodes in a network share common model parameters (common infection rate, common patching rate, etc.). Due to different node functions and different node security levels in real-world applications, these parameters may vary from node to node. Hence, heterogeneous node-based SIPS models should be considered (see Refs. [40] and [32]). Third, it is highly rewarding to study the network immunization [41–45] under the proposed model. Last, but not least, the method developed in this work can be applied to other types of malicious epidemics such as the rumor spreading [46,47].

### Acknowledgments

The authors are grateful to the three anonymous reviewers and the editor for their valuable comments and constructive suggestions that have greatly improved the quality of this paper. This work is supported by Natural Science Foundation of China (Grant Nos. 61572006, 61379158, 71301177), Science and Technology Support Program of China (Grant No. 2014BAH25F01), and Basic and Advanced Research Program of Chongqing (Grant Nos. cstc2013jcyjA1658, cstc2014jcyjA40054).

### Appendix A

For the purpose of showing Lemma 3, we need the following notations and lemmas.  
Let

$$C_1 = \beta A - \text{diag}\left(\frac{\gamma_3}{1 - I_i^*}\right),$$

$$D_1 = \gamma_1 B - \text{diag}\left(\frac{\alpha}{1 - P_i^*}\right),$$

and

$$\mathbf{G}_1 = \beta \mathbf{A} - \text{diag} \left( \frac{\gamma_3 + \gamma_1 \sum_j b_{ij} P_j^*}{1 - I_i^{**} - P_i^*} \right).$$

**Lemma 5.** Consider model (2). The following claims hold true.

- (a) If  $\rho(\mathbf{A}) > \frac{\gamma_3}{\beta}$ , then  $\mathbf{C}_1$  has  $N - 1$  negative eigenvalues and one zero eigenvalue.
- (b) If  $\rho(\mathbf{B}) > \frac{\alpha}{\gamma_1}$ , then  $\mathbf{D}_1$  has  $N - 1$  negative eigenvalues and one zero eigenvalue.
- (c) Suppose  $\gamma_1 = \gamma_2$ . If  $\rho(\mathbf{B}) > \frac{\alpha}{\gamma_1}$  and  $\rho(\mathbf{A}) > \max_i \left\{ \frac{\alpha P_i^* + \gamma_3 (1 - P_i^*)}{\beta (1 - P_i^*)^2} \right\}$ , then  $\mathbf{G}_1$  has  $N - 1$  negative eigenvalues and one zero eigenvalue.

**Proof.** (a) Let  $\mathbf{C}_2 = \max_i \left\{ \frac{\gamma_3}{1 - P_i^*} \right\} \cdot \mathbf{E}_N + \mathbf{C}_1$ . The connectedness of  $G_v$  implies the irreducibility of  $\mathbf{A}$ , which in turn implies the irreducibility of  $\mathbf{C}_2$ . According to the Perron–Frobenius Theorem [34],  $\mathbf{C}_2$  has a simple positive eigenvalue  $\rho(\mathbf{C}_2)$ , and there is a positive eigenvector  $\mathbf{w}$  belonging to  $\rho(\mathbf{C}_2)$ ,  $\mathbf{C}_2 \mathbf{w} = \rho(\mathbf{C}_2) \mathbf{w}$ . So,

$$\mathbf{C}_1 \mathbf{w} = \left\{ \rho(\mathbf{C}_2) - \max_i \left\{ \frac{\gamma_3}{1 - I_i^*} \right\} \right\} \mathbf{w}.$$

Thus,  $\mathbf{w}$  is also an eigenvector of  $\mathbf{C}_1$ . On the other hand, it follows from Theorem 1(a) that  $\mathbf{C}_1 \mathbf{1}^* = \mathbf{0}$ . So,  $\mathbf{1}^*$  is another eigenvector of  $\mathbf{C}_1$ . As  $\mathbf{w}^T \cdot \mathbf{1}^* > 0$ , we get  $\rho(\mathbf{C}_2) = \max_i \left\{ \frac{\gamma_3}{1 - I_i^*} \right\}$  and  $\rho(\mathbf{C}_1) = 0$ . Finally, the simplicity of  $\rho(\mathbf{C}_1)$  follows from the simplicity of  $\rho(\mathbf{C}_2)$ . The claim is proved.

(b) Let  $\mathbf{D}_2 = \max_i \left\{ \frac{\alpha}{1 - P_i^*} \right\} \cdot \mathbf{E}_N + \mathbf{C}_1$ . The subsequent argument is analogous to that for Claim (a).

(c) Let  $\mathbf{G}_2 = \max_i \left( \frac{\gamma_3 + \gamma_1 \sum_j b_{ij} P_j^*}{1 - I_i^{**} - P_i^*} \right) \cdot \mathbf{E}_N + \mathbf{G}_1$ . The subsequent argument is analogous to that for Claim (a). □

Let

$$\mathbf{C}_3 = \beta \mathbf{A} - \text{diag} \left( \frac{\gamma_3}{(1 - I_i^*)^2} \right),$$

$$\mathbf{D}_3 = \gamma_1 \mathbf{B} - \text{diag} \left( \frac{\alpha}{(1 - P_i^*)^2} \right),$$

and

$$\mathbf{G}_3 = \beta \mathbf{A} - \text{diag} \left( \frac{1 - P_i^*}{(1 - I_i^{**} - P_i^*)^2} \left[ \gamma_3 + \gamma_1 \sum_j b_{ij} P_j^* \right] \right).$$

**Lemma 6.** Consider model (2). The following claims hold true.

- (a)  $\mathbf{C}_3$  is negative definite if  $\rho(\mathbf{A}) > \frac{\gamma_3}{\beta}$ .
- (b)  $\mathbf{D}_3$  is negative definite if  $\rho(\mathbf{B}) > \frac{\alpha}{\gamma_1}$ .
- (c)  $\mathbf{G}_3$  is negative definite if  $\gamma_1 = \gamma_2$ ,  $\rho(\mathbf{B}) > \frac{\alpha}{\gamma_1}$ , and  $\rho(\mathbf{A}) > \max_i \left\{ \frac{\alpha P_i^* + \gamma_3 (1 - P_i^*)}{\beta (1 - P_i^*)^2} \right\}$ .

**Proof.** (a) It follows from Lemma 5(a) that for any  $N$ -dimensional vector  $\mathbf{x} \neq \mathbf{0}$ , we have

$$\mathbf{x}^T \left[ \beta \mathbf{A} - \text{diag} \left( \frac{\gamma_3}{(1 - I_i^*)^2} \right) \right] \mathbf{x} = \mathbf{x}^T \mathbf{C}_1 \mathbf{x} - \mathbf{x}^T \cdot \text{diag} \left( \frac{\gamma_3 I_i^*}{(1 - I_i^*)^2} \right) \cdot \mathbf{x} \leq -\mathbf{x}^T \cdot \text{diag} \left( \frac{\gamma_3 I_i^*}{(1 - I_i^*)^2} \right) \cdot \mathbf{x} < 0.$$

The proof is complete.

The proofs of Claims (b) and (c) are similar and hence are omitted. □

We are ready to prove Lemma 3.

**Proof of Lemma 3.** (a) Observe that  $\mathbf{M}_1 = \text{diag}(1 - I_i^*) \cdot \mathbf{C}_3$  is Metzler. It follows from Lemma 6(a) that  $\mathbf{M}_1$  is Hurwitz. The claim follows from the observation that  $\mathbf{M}_1$  has a real spectrum.

The proofs of Claims (b) and (c) are similar and hence are omitted. □

### Appendix B

**Proof of Theorem 4.** (a) It follows from the proof of Theorem 1 that

$$\phi_i(\mathbf{1}^*, \beta, \gamma_3) = -\gamma_3 I_i^* + \beta (1 - I_i^*) \sum_j a_{ij} I_j^* = 0, \quad 1 \leq i \leq N.$$

By Lemma 3(a),  $\mathbf{M}_1 = [\frac{\partial \phi_i}{\partial I_j^*}]_{N \times N}$  is invertible. By applying the Implicit Differentiation Theorem to the system, we get

$$\frac{\partial \mathbf{I}^*}{\partial \beta} = -\mathbf{M}_1^{-1} \cdot \text{diag}(1 - I_i^*) \cdot \mathbf{A} \mathbf{I}^*,$$

and

$$\frac{\partial \mathbf{I}^*}{\partial \gamma_3} = \mathbf{M}_1^{-1} \mathbf{I}^*.$$

As  $\mathbf{M}_1$  is Metzler, irreducible, and with a negative spectrum, it follows that all the entries of  $\mathbf{M}_1^{-1}$  are negative, which implies that  $\frac{\partial I_i^*}{\partial \beta} > 0$  and  $\frac{\partial I_i^*}{\partial \gamma_3} < 0$  for all  $1 \leq i \leq N$ . The proof is complete.

(b) The argument is analogous to that for Claim (a) and hence is omitted.

(c) It follows from the proof of Theorem 1 that

$$\varphi_i(\mathbf{I}^{**}, \mathbf{P}^*, \beta, \gamma_1, \gamma_3) = -\gamma_3 I_i^{**} + \beta(1 - I_i^{**} - P_i^*) \sum_j a_{ij} I_j^{**} - \gamma_1 I_i^{**} \sum_j b_{ij} P_j^* = 0, \quad i = 1, 2, \dots, N.$$

By Lemma 3(c),  $\mathbf{M}_3 = [\frac{\partial \phi_i}{\partial I_j^{**}}]_{N \times N}$  is invertible. By applying the Implicit Differentiation Theorem to the system, we get

$$\frac{\partial \mathbf{I}^{**}}{\partial \beta} = -\mathbf{M}_3^{-1} \cdot \text{diag}(1 - I_i^{**} - P_i^*) \cdot \mathbf{A} \mathbf{I}^{**},$$

$$\frac{\partial \mathbf{I}^{**}}{\partial \gamma_1} = \mathbf{M}_3^{-1} \cdot \text{diag}(I_i^*) \cdot \mathbf{B} \left[ \mathbf{P}^* + \gamma_1 \frac{\partial \mathbf{P}^*}{\partial \gamma_1} \right],$$

and

$$\frac{\partial \mathbf{I}^{**}}{\partial \gamma_3} = \mathbf{M}_3^{-1} \mathbf{I}^*.$$

As  $\mathbf{M}_3$  is Metzler, irreducible, and with a negative spectrum, it follows that all the entries of  $\mathbf{M}_3^{-1}$  are negative, which implies the claim.  $\square$

## References

- [1] Y. Wang, S. Wen, Y. Xiang, W. Zhou, Modeling the propagation of worms in networks: A survey, *IEEE Commun. Surv. Tutor.* 16 (2) (2014) 942–960.
- [2] J.O. Kephart, S.R. White, Directed-graph epidemiological models of computer viruses, in: *Proceedings of the IEEE Computer Society Symposium on Research in Security and Privacy*, 1991, pp. 343–359.
- [3] J.R.C. Piqueira, A.A. de Vasconcelos, C.E.C.J. Gabriel, V.O. Araujo, Dynamic models for computer viruses, *Comput. Secur.* 27 (7–8) (2008) 355–359.
- [4] B.K. Mishra, S.K. Pandey, Dynamic model of worms with vertical transmission in computer network, *Appl. Math. Comput.* 217 (21) (2011) 8438–8446.
- [5] J. Ren, X. Yang, Q. Zhu, L.X. Yang, C. Zhang, A novel computer virus model and its dynamics, *Nonlinear Anal. RWA* 13 (1) (2012) 376–384.
- [6] L.X. Yang, X. Yang, Q. Zhu, L. Wen, A computer virus model with graded cure rates, *Nonlinear Anal. RWA* 14 (1) (2013) 414–422.
- [7] Y. Muroya, Y. Enatsu, H. Li, Global stability of a delayed SIRS computer virus propagation model, *Int. J. Comput. Math.* 91 (3) (2014) 347–367.
- [8] C. Gan, X. Yang, W. Liu, Q. Zhu, A propagation model of computer virus with nonlinear vaccination probability, *Commun. Nonlinear Sci. Numer. Simulat.* 19 (1) (2014) 92–100.
- [9] S. Wen, W. Zhou, J. Zhang, Y. Xiang, W. Zhou, W. Jia, C.C. Zou, Modeling and analysis on the propagation dynamics of modern email malware, *IEEE Trans. Dependable Secur. Comput.* 11 (4) (2014) 361–374.
- [10] L.X. Yang, X. Yang, The impact of nonlinear infection rate on the spread of computer virus, *Nonlinear Dyn.* 82 (1–2) (2015) 85–95.
- [11] B.K. Mishra, D.K. Saini, SEIRS epidemic model with delay for transmission of malicious objects in computer network, *Appl. Math. Comput.* 188 (2) (2007) 1476–1482.
- [12] L. Feng, X. Liao, H. Li, Q. Han, Hopf bifurcation analysis of a delayed viral infection model in computer networks, *Math. Comput. Model.* 56 (7–8) (2012) 167–179.
- [13] Y. Yao, L. Guo, H. Guo, G. Yu, F. Gao, X. Tong, Pulse quarantine strategy of internet worm propagation: Modeling and analysis, *Comput. Electr. Eng.* 38 (9) (2012) 1047–1061.
- [14] L.X. Yang, X. Yang, The pulse treatment of computer viruses: a modeling study, *Nonlinear Dyn.* 76 (2) (2014) 1379–1393.
- [15] Y. Yao, X. Feng, W. Yang, W. Xiang, F. Gao, Analysis of a delayed internet worm propagation model with impulsive quarantine strategy, *Math. Probl. Eng.* 2014 (2014). Article ID 369360.
- [16] J. Amador, J.R. Artalejo, Stochastic modeling of computer virus spreading with warning signals, *J. Frankl. Inst.* 350 (5) (2013) 1112–1138.
- [17] J. Amador, The stochastic SIRA model for computer viruses, *Appl. Math. Comput.* 232 (1) (2014) 1112–1124.
- [18] L.X. Yang, X. Yang, The effect of infected external computers on the spread of viruses: A compartment modeling study, *Physica A* 392 (24) (2013) 6523–6535.
- [19] L.X. Yang, X. Yang, A novel virus-patch dynamic model, *PloS One* 10 (9) (2015) E0137858.
- [20] Q. Zhu, X. Yang, L.X. Yang, X. Zhang, A mixing propagation model of computer viruses and countermeasures, *Nonlinear Dyn.* 73 (3) (2013) 1433–1441.
- [21] M. Sun, D. Li, D. Han, C. Jia, Impact of anti-virus software on computer virus dynamical behavior, *Int. J. Mod. Phys. C* 25 (5) (2014) 1440010.
- [22] A.K. Misra, M. Verma, A. Sharma, Capturing the interplay between malware and anti-malware in a computer network, *Appl. Math. Comput.* 229 (25) (2014) 340–349.
- [23] J. Ren, Y. Xu, J. Liu, Investigation of dynamics of a virus-antivirus model in complex network, *Physica A* 421 (1) (2015) 533–540.
- [24] A.M. Rey, Mathematical modeling of the propagation of malware: A review, *Secur. Comm. Netw.* 8 (2015) 2561–2579.
- [25] P.V. Mieghem, J. Omic, R. Kooij, Virus spread in networks, *IEEE/ACM Trans. Netw.* 17 (1) (2009) 1–14.
- [26] S. Xu, W. Lu, Z. Zhan, A stochastic model of multivirus dynamics, *IEEE Trans. Dependable Secur. Comput.* 9 (1) (2012) 30–45.
- [27] F.D. Sahneh, C. Scoglio, Optimal information dissemination in epidemic networks, in: *Proceedings of the 50th IEEE Conference on Decision Control*, 2012.

- [28] M. Youssef, C. Scoglio, An individual-based approach to SIR epidemics in contact networks, *J. Theory Biol.* 283 (2011) 136–144.
- [29] Y. Lin, J.C. Lui, Modelling multi-state diffusion process in complex networks: theory and applications, *J. Comp. Netw.* 2 (4) (2014) 431–459.
- [30] C. Nowzari, V.M. Preciado, G.J. Pappas, Stability analysis of generalized epidemic models over directed networks, in: *Proceedings of the 53rd IEEE Conference on Decision and Control*, 2014.
- [31] L.X. Yang, M. Draief, X. Yang, The impact of the network topology on the viral prevalence: a node-based approach, *PLoS One* 10 (7) (2015) E0134507.
- [32] L.X. Yang, M. Draief, X. Yang, Heterogeneous virus propagation in networks: A theoretical study, *Math. Meth. Appl. Sci.* (2016a), doi:10.1002/mma.4061.
- [33] J.A. Yorke, Invariance for ordinary differential equations, *Theory Comput. Syst.* 1 (1967) 353–372.
- [34] R. Bhatia, *Matrix Analysis*, Springer-Verlag, New York, USA, 2011.
- [35] E. Shamash, *Fixed Point Theory: Banach, Brouwer and Schauder Theorems*, LAP Lambert Academic Publishing, Saarbrücken, Germany, 2010.
- [36] R.C. Robinson, *An Introduction to Dynamical Systems: Continuous and Discrete*, American Mathematical Society: Providence, USA, 2012.
- [37] L. Markus, Asymptotically autonomous differential systems, in: S. Lefschetz (Ed.), *Contributions to the Theory of Nonlinear Oscillations III*, *Annals of Mathematics Studies*, 36, Princeton University Press, Princeton, 1956, pp. 17–29.
- [38] A.-L. Barabási, R. Albert, Emergence of scaling in random networks, *Science* 286 (5439) (1999) 509–512.
- [39] D. Watts, S. Strogatz, Collectivedynamics of small-world networks, *Nature* 393 (6684) (1998) 440–442.
- [40] P.V. Mieghem, J. Omic, In-homogeneous virus spread in networks, 11 July 2014, arXiv:1306.2588 [math.OC].
- [41] V.M. Preciado, M. Zargham, C. Enyioha, A. Jadbabaie, G.J. Pappas, Optimal resource allocation for network protection against spreading processes, *IEEE Trans. Control Netw. Syst.* 1 (1) (2014) 99–108.
- [42] H. Shakeri, F.D. Sahneh, C. Scoglio, Optimal information dissemination strategy to promote preventive behaviours in multilayer epidemic networks, *Math. Biosci. Eng.* 12 (3) (2015) 609–623.
- [43] A. Khanafar, T. Basar, An optimal control problem over infected networks, in: *Proceedings International Conference Control Dynamic Systems Robotics*, Ottawa, Ontario, Canada, 2014.
- [44] S. Eshghi, M. Khouzani, S. Sarkar, S. Venkatesh, Optimal patching in clustered malware epidemics, *IEEE/ACM Trans. Netw.* 24 (1) (2014) 283–298.
- [45] L.X. Yang, M. Draief, X. Yang, The optimal dynamic immunization under a controlled heterogeneous node-based SIRS model, *Physica A* 450 (2016) 403–415.
- [46] S. Wen, J. Jiang, Y. Xiang, S. Yu, W. Zhou, W. Jia, To shut them up or to clarify: Restraining the spread of rumors in online social networks, *IEEE Trans. Parallel Distrib. Syst.* 25 (12) (2014) 3306–3316.
- [47] S. Wen, M. Haghghi, C. Chen, Y. Xiang, W. Zhou, W. Jia, A sword with two edges: propagation studies on both positive and negative information in online social networks, *IEEE Trans. Comput.* 64 (3) (2015) 640–653.